

Luminescence Properties of Yttrium Borate Samples with the Morphologies Controlled by Solvothermal Method

Saburo Hosokawa and Masashi Inoue*

Department of Energy and Hydrocarbon Chemistry, Graduate School of Engineering,
Kyoto University, Katsura, Kyoto 615-8510

(Received July 9, 2009; CL-090647; E-mail: inoue@scl.kyoto-u.ac.jp)

Solvothermal reaction of yttrium chloride hydrate and trimethoxyborane in 1,4-butanediol in the presence of amines at 315 °C directly yielded YBO_3 crystals having flower-like morphology (particle size; 3–8 μm). The crystal growth toward the c axis was inhibited by adsorption of amines on the ab plane, and plate-like crystals were formed. The luminescence chromaticity of $\text{Y}_{0.9}\text{Eu}_{0.1}\text{BO}_3$ samples synthesized by solvothermal reaction was different from that prepared by solid-state reaction; samples synthesized by the solvothermal reaction exhibited larger relative intensity ratio of the emission at 580 nm to that at 610 nm than samples prepared by the solid-state reaction.

Europium-doped rare earth borate with vaterite structure, in particular $(\text{Gd}, \text{Y})\text{BO}_3:\text{Eu}^{3+}$, emits red color and represents an important material as a phosphor for plasma display panels.¹ One problem is that the orange emission is stronger than the red. The luminescence properties of phosphor materials are strongly affected by the particle size and morphology.^{2,3} It has been reported that nanosized or nano-sheet $\text{YBO}_3:\text{Eu}^{3+}$ samples show enhanced intensity of the red emission.² However, the relationships between morphology and photoluminescence property have not been systematically investigated.

Solvothermal method are reactions in a liquid medium at higher temperatures,⁴ and reaction in water at high temperatures in a closed vessel is called hydrothermal reaction. We refer to similar reactions in glycol as glycolthermal reaction. We have shown various crystalline oxides or mixed oxides can be synthesized by the glycolthermal method.⁵ In a previous work, we found that YBO_3 having a spheroidal morphology with a diameter of 1 μm was synthesized by glycolthermal reaction of yttrium acetate and trimethoxyborane in 1,4-butanediol.⁶

In the present work, the morphology of YBO_3 was controlled by the addition of amines to the reaction system, and luminescence properties of 10% Eu-doped YBO_3 ($\text{YBO}_3:\text{Eu}$) thus-synthesized were investigated.

Trimethoxyborane (12.5 mmol) and yttrium chloride hexahydrate (12.5 mmol) were suspended in 100 mL of 1,4-butanediol in a test tube, and an amine ($\text{N}/\text{Cl} = 5$) was added to the tube, which was then set in a 300-mL autoclave. An additional 40 mL of 1,4-butanediol and 5 mL of the amine were placed in the gap between the autoclave wall and the test tube. Butylamine (BA), hexylamine (HA), and ethylenediamine (EDA) were predominantly used as the amines. The autoclave was purged with nitrogen, heated to 315 °C at a rate of 2.3 °C min⁻¹, and kept at that temperature for 2 h. After the assembly was cooled to room temperature, the resulting products were centrifuged. The product was washed with methanol and water. The samples synthesized from yttrium acetate and yttrium chloride are designated as P1 and P2, respectively. If amines were added to the reaction medium, these notations are followed by abbreviation of the amine in parentheses. For example, P1(HA) means the product obtained by the reaction of yttrium acetate and trimethoxyborane in 1,4-butanediol in the presence of HA. For the synthesis of $\text{YBO}_3:\text{Eu}$, europium acetate tetrahydrate was used for P1, and europium chloride hexahydrate for P2. X-ray powder diffraction (XRD, Shimadzu XD-D1) was recorded using Cu K α radi-

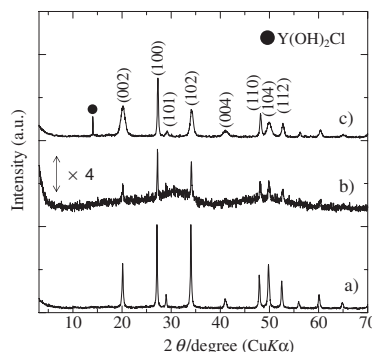


Figure 1. XRD patterns of: a) P1, b) P1(HA), and c) P2(HA).

ation. The morphology of the products was observed with a scanning electron microscope (SEM, Hitachi S-2500CX). The luminescence spectra of $\text{YBO}_3:\text{Eu}$ were recorded under 240-nm excitation on a Shimadzu RF-5300PC spectrophotofluorometer.

Figure 1 shows the XRD patterns of some of the products. Although P1 had a high crystallinity, the addition of HA inhibited the crystallization of YBO_3 (Figure 1b). On the other hand, well-crystallized YBO_3 was obtained for P2(HA) although the sample was contaminated with a small amount of $\text{Y}(\text{OH})_2\text{Cl}$.⁷ Since YCl_3 has a higher solubility in 1,4-butanediol than $\text{Y}(\text{OAc})_3$, the crystallization of YBO_3 easily proceeded in the solvothermal reaction of YCl_3 even in the presence of amines. Note that the 00l diffraction peaks were broader than $hk0$ peaks for P2(HA). The SEM image (Figure S1)⁸ showed that P1 comprised monodispersed spheroidal particles with a diameter of 1 μm .⁶ P2(HA) was composed of well-dispersed flower-like particles with particle sizes of about 3–5 μm . The particle sizes were distributed in a narrow range, indicating monodispersed particles were formed (Figure S2).⁸ The high-magnification SEM image showed that each particle was made by aggregation of plate-like crystals (Figure 2). These results indicate that the crystal growth toward the c axis was inhibited by the adsorption of amines on the ab plane, yielding plate-like crystals.

Figure 2 also shows the morphologies of P2(BA) and P2(EDA). Although the XRD pattern of P2(EDA) was essentially identical with those of P2(HA) and P2(BA), the aggregation state of plate particles in P2(EDA) was different from that in P2(HA) or P2(BA). For P2(EDA), a large number of small plate particles were aggregated yielding 3–6- μm flower-like secondary particles. Therefore, the size of plate-like crystals and their aggregation state could be controlled by the amine used.

In the presence of amines such as dipropylamine, triethylamine, and oleylamine with high steric hindrance, irregularly shaped YBO_3 particles were obtained, while n -alkylamines such as BA, octylamine, decylamine, and dodecylamine gave particles made by aggregation of plate-like particles (Figures S1 and S2).⁸ In the case of diamines, particles with flower-like morphology were obtained for EDA and 1,8-octanediamine, while 1,4-butanediamine and 1,6-hexanediamine gave irregularly shaped YBO_3 particles (Figures S1 and S2).⁸

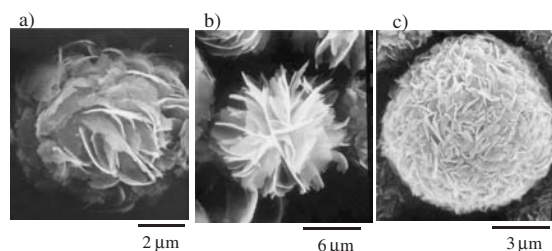


Figure 2. SEM images of: a) P2(HA), b) P2(BA), and c) P2(EDA).

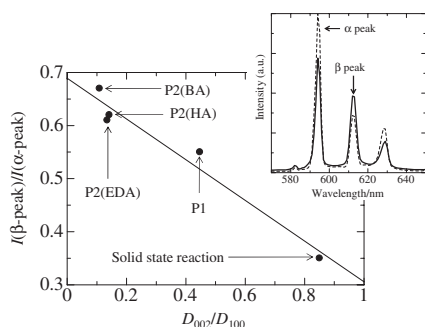


Figure 3. Relationship between the ratio of $I(\beta\text{-peak})/I(\alpha\text{-peak})$ and the D_{002}/D_{100} , and emission spectra under 240-nm UV excitation of $\text{YBO}_3\text{:Eu}$ synthesized by solid-state reaction^a (broken line) and P2(BA) (solid line). ^aSynthesized from Y_2O_3 , Eu_2O_3 , and H_3BO_3 at 1100 °C for 3 h.

The luminescence spectrum of $\text{YBO}_3\text{:Eu}$ synthesized under the conditions adopted for synthesis of P2(BA) is shown in the inset of Figure 3. The peaks observed at 580–720 nm are due to the transitions from excited $^5\text{D}_0$ level to $^7\text{F}_J$ ($J = 1\text{--}4$) levels of Eu^{3+} .² The peaks at 590 (orange emission) and 610 nm (red emission) are designated as α - and β -peaks, respectively, and the intensity ratios of β -peak to α -peak, $I(\beta\text{-peak})/I(\alpha\text{-peak})$, of the solvothermally synthesized products, were much larger than that of the sample prepared by solid-state reaction (Figure S3).⁸ As shown in Figure 3, the $I(\beta\text{-peak})/I(\alpha\text{-peak})$ ratio increased with the decrease in the relative crystallite size ratio (D_{002}/D_{100}) calculated from 002 and 100 diffraction peaks of the plate crystals,⁸ indicating that the high $I(\beta\text{-peak})/I(\alpha\text{-peak})$ ratio was observed for YBO_3 crystals preferentially grown along the ab plane.

Mahiou et al. reported that the crystal structure of YBO_3 is in the $P6_3/m$ space group, in which yttrium atoms occupy a site with a point symmetry of S_6 .⁹ However, each yttrium atom is coordinated with eight oxygen atoms in a trigonal bipyramidal antiprism structure. Of eight oxygen atoms, two oxygen atoms are located in Wyckoff $6h$ sites with $1/3$ occupancy. Therefore, the actual point symmetry of the rare earth element is much lower than S_6 . Wei et al. examined the effect of particle size on chromaticity of $\text{YBO}_3\text{:Eu}$ and reported that the unit cell parameter ratio, c/a , decreased with the decrease in particle size.² They attributed the high $I(\beta\text{-peak})/I(\alpha\text{-peak})$ ratio observed for the samples with smaller particle size to this lattice distortion. In the present study, the samples that exhibited high $I(\beta\text{-peak})/I(\alpha\text{-peak})$ had large a values, in agreement with the tendency reported by Wei et al.² However, expansion or constriction of the lattice does not alter the local symmetry of the rare earth sites; therefore, this point is not the origin of the enlarged $I(\beta\text{-peak})/I(\alpha\text{-peak})$ ratio because Judd–Ofelt theory predicts that the high ratio of $I(\beta\text{-peak})/I(\alpha\text{-peak})$ is caused by the low crystal field symmetry.¹⁰ Wei et al. also pointed out the possibility that the disordered Eu sites on the sur-

Table 1. Crystallite size, BET surface area and $I(\beta\text{-peak})/I(\alpha\text{-peak})$ of $\text{YBO}_3\text{:Eu}$

Sample	Crystallite size/nm		D_{002}/D_{001}	BET surface area /m ² g ⁻¹	$I(\beta\text{-peak})/I(\alpha\text{-peak})$
	(002)	(100)			
P2(BA)	9	86	0.10	37	0.67
P2(BA) ^a	12	69	0.17	—	0.76
P2(BA) ^b	101	179	0.56	—	0.51
P2(EDA)	7	49	0.14	52	0.61
P2(HA)	11	77	0.14	31	0.62
P1	63	141	0.45	9	0.55
Solid state reaction	120	142	0.85	4	0.35

^aThe sample was obtained by calcination of P(BA) at 800 °C. ^bThe sample was obtained by calcination of P(BA) at 1100 °C.

face of crystals may contribute to the enhanced $I(\beta\text{-peak})/I(\alpha\text{-peak})$ ratio.² However, the surface area of $\text{YBO}_3\text{:Eu}$ did not correlate with the $I(\beta\text{-peak})/I(\alpha\text{-peak})$ ratio (Table 1). Therefore, we proposed the following scenario: Preferential growth of the crystals toward ab directions gave thin crystals, which are easily curved as shown in Figure 2. Curved crystals lower the local symmetry of Eu^{3+} sites, thus causing the enhanced $I(\beta\text{-peak})/I(\alpha\text{-peak})$ ratio. Since the crystallite size and $I(\beta\text{-peak})/I(\alpha\text{-peak})$ ratio of the sample obtained by calcination of P2(BA) at 800 °C were essentially identical with those of as-synthesized P2(BA), the organic species remaining on as-synthesized P2(BA) particles did not affect the $I(\beta\text{-peak})/I(\alpha\text{-peak})$ ratio. Growth of the YBO_3 crystals occurred by the calcination at 1100 °C, and the $I(\beta\text{-peak})/I(\alpha\text{-peak})$ ratio increased, but the luminescence intensity drastically increased (Figure S4).⁸

In summary, the aggregation and morphology of plate crystals of YBO_3 can be controlled by the addition of amine to the solvothermal reaction. The ratio of $I(\beta\text{-peak})/I(\alpha\text{-peak})$ of $\text{YBO}_3\text{:Eu}$ was controlled by the morphology of YBO_3 crystals.

This work was supported by Grant-in-Aid for Scientific Research (No. 19018012) from the Ministry of Education, Cultures, Sports, Science and Technology, Japan.

References and Notes

- C. R. Ronda, T. Jüstel, H. Nikol, *J. Alloys Compd.* **1998**, 275–277, 669.
- Z. Wei, L. Sun, C. Liao, J. Yin, X. Xiaocheng, C. Yan, S. Lü, *J. Phys. Chem. B* **2002**, 106, 10610; X.-C. Jiang, L.-D. Sun, C.-H. Yan, *J. Phys. Chem. B* **2004**, 108, 3387.
- S. Lemanceau, G. Bertrand-Chadeyron, R. Mahiou, M. El-Ghozzi, J. C. Cousseins, P. Conflant, R. N. Vannier, *J. Solid State Chem.* **1999**, 148, 229; M. Tukia, J. Hölsä, M. Lastusaari, J. Niittykoski, *Opt. Mater.* **2005**, 27, 1516; D.-S. Kim, R.-Y. Lee, *J. Mater. Sci.* **2000**, 35, 4777; D. Boyer, G. Bertrand-Chadeyron, R. Mahiou, L. Lou, A. Brioude, J. Mugnier, *Opt. Mater.* **2001**, 16, 21.
- M. Inoue, in *Chemical Processing of Ceramics*, 2nd ed., ed. by B. Lee, S. Komanneni, Taylor & Francis, Boca Raton, FL, **2005**, Chap. 2, pp. 22–63.
- M. Inoue, M. Kimura, T. Inui, *Chem. Commun.* **1999**, 957; M. Inoue, H. Otsu, H. Kominami, T. Inui, *J. Am. Ceram. Soc.* **1991**, 74, 1452; M. Inoue, T. Nishikawa, H. Otsu, H. Kominami, T. Inui, *J. Am. Ceram. Soc.* **1998**, 81, 1173.
- S. Hosokawa, Y. Tanaka, S. Iwamoto, M. Inoue, *J. Mater. Sci.* **2008**, 43, 2276.
- S. Hosokawa, S. Iwamoto, M. Inoue, *J. Alloys Compd.* **2006**, 408–412, 529.
- Supporting Information is available electronically on the CSJ-Journal Web site, <http://www.csj.jp/journals/chem-lett/index.html>.
- G. Chadeyron, E. El-Ghozzi, R. Mahiou, A. Arbus, J. C. Cousseins, *J. Solid State Chem.* **1997**, 128, 261; D. Boyer, G. Bertrand, R. Mahiou, *J. Lumin.* **2003**, 104, 229.
- B. R. Judd, *Phys. Rev.* **1962**, 127, 750.